Nuclear Magnetic Resonance Studies of Resorcinol−Formaldehyde Aerogels

Igor L. Moudrakovski,* Christopher I. Ratcliffe, and John A. Ripmeester

Steacie Institute for Molecular Sciences, National Research Council, Ottawa, Ontario, Canada K1A 0R6

Li-Qiong Wang* and Gregory J. Exarhos

Material Science Department, Pacific Northwest National Laboratory, Richland, Washington 99354

Theodore F. Baumann and Joe H. Satcher

Chemistry and Material Science Directorate, Lawrence Livermore National Laboratory, Livermore, California 94550

Received: February 3, 2005; In Final Form: April 14, 2005

In this article, we report a detailed study of resorcinol−formaldehyde (RF) aerogels prepared under different processing conditions, [resorcinol]/[catalyst] (R/C) ratios in the starting sol−gel solutions, using continuous flow hyperpolarized ^{129}Xe NMR in combination with solid-state ^{13}C and two-dimensional wide-line separation (2D-WISE) NMR techniques. The degree of polymerization and the mobility of the cross-linking functional groups in RF aerogels are examined and correlated with the R/C ratios. The origin of different adsorption regions is evaluated using both coadsorption of chloroform and 2D EXSY ^{129}Xe NMR. A hierarchical set of Xe exchange processes in RF aerogels is found using 2D EXSY ^{129}Xe NMR. The exchange of Xe gas follows the sequence (from fastest to slowest): mesopores with free gas, gas in meso- and micropores, free gas with micropores, and, finally, among micropore sites. The volume-to-surface-area (V_g/S) ratios for aerogels are measured for the first time without the use of geometric models. The V_g/S parameter, which is related both to the geometry and the interconnectivity of the pore space, has been found to correlate strongly with the R/C ratio and exhibits an unusually large span: an increase in the R/C ratio from 50 to 500 results in about a 5-fold rise in V_g/S.

Introduction

Organic aerogels are novel open-pore materials with very high surface areas (up to 1000 m^2/g) and pores of nanometer size (3−25 nm).[1−4] They exhibit extremely low mass densities, low thermal conductivity, good acoustic insulation, and low dielectric constants. These materials have potential applications in catalysis, advanced separation techniques, energy storage, environmental remediation, and as insulating materials. Organic aerogels are stiffer and stronger than silica aerogels and demonstrate better insulating properties.[5]

Resorcinol−formaldehyde (RF) aerogels are typically prepared through the base-catalyzed sol−gel polymerization of resorcinol with formaldehyde in aqueous solution to produce gels, which are then dried in supercritical CO_2.[1−4] The [resorcinol]/[catalyst] (R/C) ratio in the starting sol−gel solution has been found to be the dominant factor that affects the properties of RF aerogels. With high catalyst concentrations (i.e., R/C = 50), TEM shows that the particles that comprise the aerogel framework have diameters of ∼3 nm and are joined together with large necks, giving the aerogel a "polymeric" appearance. With low catalyst concentrations (i.e., R/C = 300), the resultant aerogels exhibit a "colloidal" microstructure, consisting of larger particles (16−20 nm) connected by smaller necks. These microstructural features have a profound effect on the bulk physical properties (i.e., surface area and mechanical strength) of the aerogel. As a result, the "polymeric" RF aerogels possess higher surface areas and compressive moduli as compared to the "colloidal" RF aerogels. Since the unique microstructures of aerogels are responsible for their unusual properties, characterizing the detailed pore structures and correlating them with the processing parameters are vital steps to establish rational design principles for novel organic aerogels with tailored properties.

Although the pore size, pore volume, and surface area are, in principle, accessible from X-ray powder diffraction, transmission electron microscopy, and nitrogen sorption, the connectivity and the structure of the pores remain unknown. In our recent communication, we reported the first use of hyperpolarized (HP) ^{129}Xe NMR to probe the geometry and interconnectivity of pores in RF aerogels and to correlate these features with the synthetic conditions.[6] Our work has demonstrated that HP ^{129}Xe NMR is so far the only method for accurately measuring the free volume-to-surface-area (V_g/S) ratios for soft mesoporous materials without using any geometric models. In this paper, we present a detailed study of RF aerogels characterized using a variety of NMR techniques with the emphasis on results that were not reported in the previous communication.[6]

The use of optical pumping techniques for the production of hyperpolarized (HP) xenon allows a dramatic increase in the sensitivity of ^{129}Xe NMR.[7] With HP xenon produced in continuous flow (CF), the technique works at very low concentrations of xenon, which makes the contribution to the chemical shift of Xe−Xe interactions on the surface very small. The observed ^{129}Xe chemical shifts can be assigned mainly to the interactions between the xenon atoms and the surface and provide information on pore structure and connectivity. The use of HP xenon is critical in ^{129}Xe NMR studies of aerogels because

* To whom correspondence should be addressed.

10.1021/jp050610r CCC: $30.25
Published on Web 05/17/2005

the extremely low densities of aerogels and very long ^{129}Xe relaxation times would otherwise result in very low signal intensities. Temperature-dependent chemical shift spectra and 2D exchange spectroscopy (EXSY) CF ^{129}Xe NMR were used to obtain a better understanding of the pore structure, the uniformity of the adsorption regions, and the interconnectivity between different adsorption regions.

Complementary to ^{129}Xe NMR, solid-state ^{13}C and two-dimensional wide-line separation (2D-WISE) NMR techniques were applied to study aerogels with different R/C ratios and to correlate the R/C ratios with the degree of polymerization and the mobility of the cross-linking functional groups. Both liquid-state and solid-state ^{13}C NMR spectra have been used to study the reaction mechanism and the chemical structures of RF aerogels previously.[2,8,9] The ^{13}C NMR relaxation times were used to monitor the degree of interparticle cross-link density in RF aerogels. A larger fraction of surface groups were cross-linked in the "polymeric" RF aerogel synthesized at R/C = 50 as compared with the "colloidal" RF aerogel synthesized at R/C = 200.[2] The mobility of methylene bridges in RF aerogels was examined using 2D WISE NMR spectroscopy developed by Spiess and co-workers.[10,11] Because of the limited chemical shift range, one-dimensional ^{1}H NMR measurements alone are insufficient to distinguish the proton signals in different chemical environments in the solid state. In 2D WISE NMR, the proton line-widths associated with the individual carbon sites can be resolved by acquiring the ^{1}H spectrum in one dimension and the high-resolution ^{13}C CP MAS spectrum in the other dimension.

Experimental Section

Materials. The preparation of RF aerogels has been described previously.[1] For each RF aerogel prepared for this study, resorcinol (1.23 g, 11.2 mmol) and formaldehyde (1.79 g, 22 mmol) were mixed in 6 mL of water, and an appropriate amount of sodium carbonate (R/C = 50, 100, 200, 300, and 500) was used as the base catalyst. The RF solution was then poured into glass vials, sealed, and cured for 7 days at 80 °C. The wet RF gels were washed with acetone until the water was completely exchanged and then dried with supercritical CO_2 (T_c = 31.1 °C, P_c = 7.4 MPa). The target density for the above formulation is 0.2 g/cm^3 and the actual densities for the RF aerogels ranged from 0.19 to 0.25 g/cm^3. The surface area and pore volume were determined by the Brunauer−Emmett−Teller (BET) method using an ASAP 2000 Surface Area Analyzer (Micromeritics Instrument Corporation). Samples of approximately 0.1 g were heated to 150 °C under vacuum (10^{-5} Torr) for at least 24 h to remove any adsorbed species. Nitrogen adsorption data were then taken at five relative pressures from 0.05 to 0.20 (relative to the saturation pressure) at 77 K to calculate the surface area and pore volume using BET methods.[12] In addition to the nitrogen adsorption measurements we have also obtained room temperature adsorption isotherms of xenon on RF aerogels with different R/C ratios. A standard volumetric adsorption system was used in these experiments with a range of Xe pressure between 10 and 1000 KPa. In this range of pressure the isotherms can be satisfactorily approximated with a Langmuir type of isotherm $\Theta = bap/(1 + bp)$, where p is the gas pressure and a and b are the adsorption capacity and equilibrium constant of adsorption, respectively. The experimental isotherms for materials with different R/C ratios are summarized in Figure 1. Physical properties including surface areas, pore volumes, parameters a and b for a series of RF aerogels prepared with the same target density formulation (0.2 g/cm^3) for five different R/C ratios are given in Table 1.

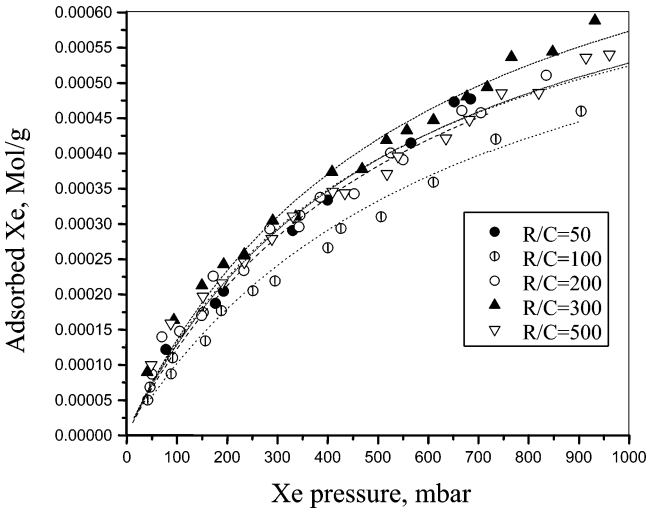

Figure 1. Xe adsorption isotherms for materials with different R/C ratios, T=293K.

TABLE 1: Adsorption Properties of RF Aerogels Used in the Study

R/C	surface area, m^2/g	total pore volume, cm^3/g	adsorption capacity for Xe a, mol/m^2	equilibrium constant for Xe adsorption b, Pa^{1-}
50	660 ± 50	2.2 ± 0.3	1.24×10^{-6}	1.73×10^{-5}
100	586 ± 10	1.6 ± 0.2	1.26×10^{-6}	1.51×10^{-5}
200	507 ± 50	3.3 ± 0.4	1.56×10^{-6}	1.96×10^{-5}
300	487 ± 50	3.5 ± 0.4	1.85×10^{-6}	1.73×10^{-5}

Solid-State^{13}c and 2D WISE NMR Measurements. Solid state ^{13}C MAS (magic angle spinning) NMR experiments were carried out with a Chemagnetics spectrometer (magnetic field 7.05 T, resonance frequency 75.0 MHz) using a variable temperature double-resonance probe. For ^{13}C NMR experiments, both single-pulse (SP) Bloch-decay and cross-polarization (CP) methods were used with ^{1}H decoupling. Samples were loaded into 7-mm Zirconia PENCIL rotors and spun at 3−4 kHz. SP spectra were collected with a 4.5-μs (90°) ^{13}C pulse, and a repetition delay of 10−60 s. The number of transients was 1000−3000. ^{13}C NMR chemical shifts were referenced to tetramethylsilane at 0 ppm

Two-dimensional wide-line separation NMR spectra were taken with the 2D WISE pulse sequence.[10] A ^{1}H 90° pulse was applied, followed by an incremented proton evolution period t_1. After each t_1 period, cross polarization (CP) pulses were followed by a TOSS (total suppression of spinning sidebands) sequence.[13] The subsequent carbon detection with proton decoupling gives a modulated ^{13}C spectrum as a function of t_1 because of the free induction decay of the associated protons. The two-dimensional Fourier transform gives a 2D spectrum with high-resolution ^{13}C CP MAS spectra in one dimension and the proton wide-line spectra associated with each carbon in the other dimension. In our measurements, a 90° pulse width for both ^{1}H and ^{13}C pulses was 4.5 μs. The ^{13}C CP MAS spectra were taken with a contact time of 0.15 ms and a pulse delay of 3s. The 2D data size was 128 points in the t_1 (^{1}H) dimension and 1000 in the t_2 (^{13}C) dimension. The spectral width in t_1 was 200 kHz (dwell time − 5 μs) and 20 kHz in t_2 (dwell time 50 μs). Amplitude spectra were used for the proton dimension (^{1}H).

^{129}Xe NMR Measurements. All ^{129}Xe NMR measurements were performed on a Bruker DSX-400 instrument at the resonance frequency of 110.7 MHz (magnetic field of 9.4 T). A solid-state multinuclear probe from Morris Instrument Inc.

modified for continuous flow experiments was used throughout this work. Variable temperature NMR experiments in the 120−400 K range were performed using a Bruker BVT3000 temperature controller. Most spectra were acquired using a simple Bloch decay pulse sequence with the delays between consecutive scans set long enough that the relative intensities of the signals did not change with the delay. 2D-EXSY spectra were obtained using standard sequences described elsewhere.[14−19] The reported ^{129}Xe NMR chemical shifts were referenced to xenon gas extrapolated to zero pressure. The temperature inside the NMR coil in our CF probe was calibrated using the ^{207}Pb resonance in $Pb(NO_3)_2$.[20]

The continuous flow (CF) system for production of hyperpolarized (HP) xenon has been described elsewhere[21] and provided 8−10% polarization of the Xe with a 30W diode laser from OptoPower Inc. A xenon−helium−nitrogen mixture with a volume composition of 1%−98%−1% was used in all of the CF HP experiments. The flow rate was monitored with a Vacuum General flow controller (model 80-4) and kept constant in the range of 40−50 scc/min (scc/min, gas flow normalized to standard conditions). In situ coadsorption of Xe and chloroform was performed by passing He gas through a saturator flask filled with $CHCl_3$ and then combining the resulting stream with the HP Xe mixture. The concentration of $CHCl_3$ in the flow is controlled by the temperature of the saturator and by adjusting the fraction of inflowing $CHCl_3$/He mixture in the total flow. Variable pressure experiments were performed using hyperpolarized xenon which had been accumulated cryogenically after the polarizer and then thawed into a transfer line connected to a cell with preevacuated aerogel. The setup for these experiments was described in detail in ref 22. The reported pressure of Xe in these experiments is not its partial pressure in the gas mixture but the actual measured pressure of pure Xe over the aerogel.

Before the NMR experiments, blocks of as-prepared RF aerogels were broken into chunks of 2−4 mm, which were then heated overnight in a flow of He at 100 °C to remove residual moisture.

Results and Discussion

Solid-State ^{13}C and 2D-WISE NMR. Organic aerogels were produced under alkaline conditions (Na_2CO_3) from the polymerization reactions of resorcinol (1,3-dihydroxy benzene) with formaldehyde. Because of the electron-donating and ortho, para-directing effect of the attached hydroxyl groups, resorcinol is particularly reactive, serving as a trifunctional monomer capable of adding formaldehyde in the 2, 4, and 6 ring positions.[1] As a result of addition and condensation reactions, aerogel products are cross-linked polymers containing methylene ($-CH_2-$) and methylene ether ($-CH_2-O-CH_2-$) bridges linking two adjacent rings. Figure 2 displays a series of solid-state ^{13}C NMR spectra of RF aerogels prepared with R/C ratios at 50, 200, and 500. Several broad resonances are observed from 160 to 0 ppm. Based on a previous NMR study,[2] we assign the resonances centered at 150, 117, 60, and 24 ppm to aromatic carbons directly attached to an −OH, aromatic carbons not directly attached to an −OH, methylene ether carbons adjacent to oxygen, and the methylene carbons, respectively. In fact there are two unresolved peaks, at 120 and 114 ppm, which constitute the broad resonance centered at 117 ppm. Similarly, a sharp peak at 29 ppm clearly emerges from a broad resonance centered at 24 ppm at a R/C ratio of 500.

Since, in the course of aqueous polycondensation, resorcinol is capable of adding formaldehyde in the 2-, 4-, and 6- ring positions, a mixture of mono-, di-, and trihydroxymethyl resorcinols are formed. These substituted resorcinol rings condense with each other to form nanometer-sized clusters in solution. Eventually, the clusters cross-link through their surface groups (e.g., $-CH_2OH$) to form a gel. Therefore, the final aerogels contain a mixture of the resorcinol rings having one, two, or three linkages to the adjacent rings. The average number of linkages per resorcinol ring depends on the degree of polymerization and condensation, which is largely controlled by the R/C ratios. The large width of the signals centered at 24 and 117 ppm is likely a result of inhomogeneity of the linkages among resorcinol rings. The emerging sharper peak at 29 ppm and the overall narrowing of the signal centered at 24 ppm can be due to a reduction in the number of the $-CH_2-$ linkages per resorcinol ring. This reduction is also reflected in the changes of the signal centered at 117 ppm. The reduced line width and the increased intensity of the 120 ppm peak is accompanied by a drop in the 114 ppm signal intensity at an increased R/C ratio. By normalizing the spectra using the area of the peak at 160 ppm, we found that the normalized peak area for the resonance centered at 24 ppm decreases with increasing R/C ratio (see insert in Figure 2). Since the normalized peak area of 24 ppm is directly proportional to the number of linkages per resorcinol ring, or to the degree of cross-linking in the aerogels, our solid-state ^{13}C NMR results suggest that aerogels prepared with a higher R/C ratio have a lower degree of cross-linking, in agreement with previous studies[1−4] where a "polymeric" RF aerogel observed using TEM was produced with a low R/C ratio. Thus, our study has demonstrated that the solid-state ^{13}C NMR can be used to systematically monitor the degree of cross-linking in aerogels prepared with different R/C ratios.

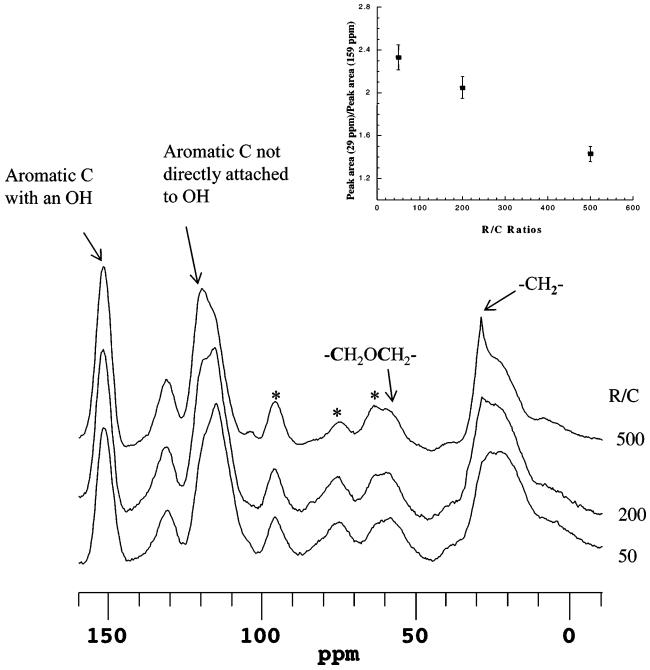

Figure 2. Series of solid-state ^{13}C NMR spectra of RF aerogels prepared with R/C ratios at 50, 200, and 500. The insert shows the peak area for the resonance centered at 24 ppm relative to that of the peak at 160 ppm as a function of R/C ratio.

2D-WISE NMR. Figure 3 shows 2D WISE NMR spectra for aerogels prepared with R/C ratios of 50, 200, 500, and their corresponding slices in the ^{1}H dimension for methylene linkage carbons ($-CH_2-$) centered at 24 ppm. 2D WISE NMR spectroscopy is used here to examine changes in the mobility of these linkage carbons in aerogels prepared with different R/C

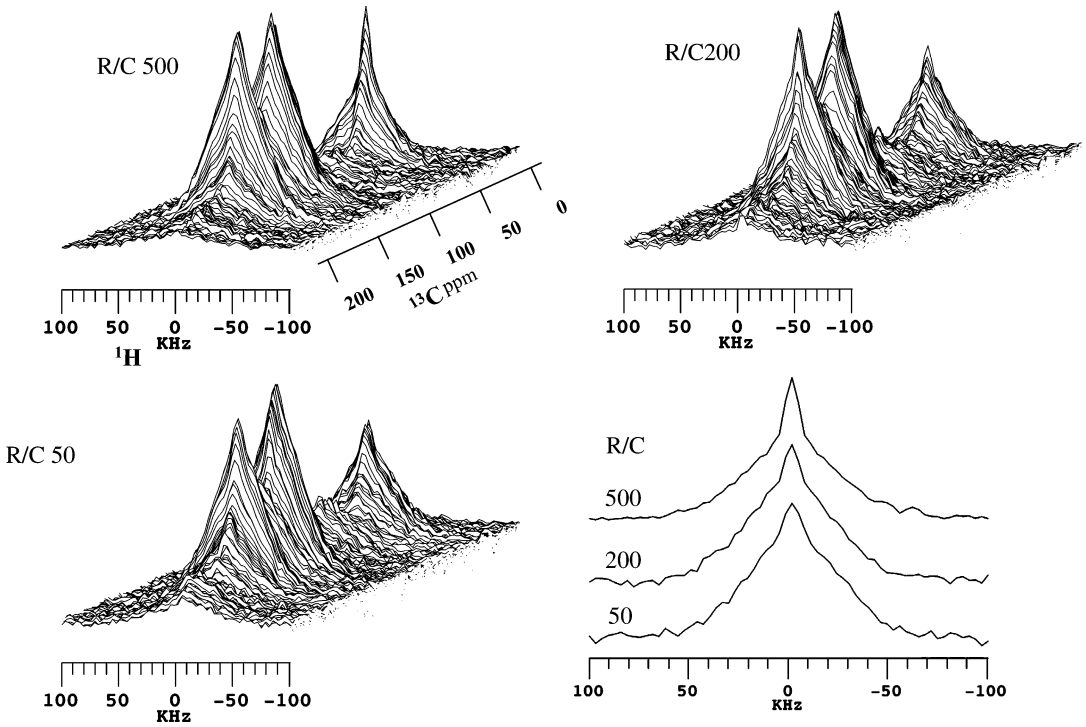

Figure 3. 2D WISE NMR spectra for aerogels prepared with R/C ratios of 50, 200, 500, and their corresponding slices in the ^{1}H dimension for methylene linkage carbons ($-CH_2-$) centered at 24 ppm.

ratios. Since in diamagnetic solids proton line-widths determined from 2D WISE NMR measurements are determined by the dipolar couplings among the ^{1}H spins, they are also sensitive to the mobility of the specific proton-bearing carbon groups. In solids containing mainly rigid methylene groups, line widths typically range from 50 to 70 kHz. These proton line-widths are significantly smaller in the presence of sufficiently rapid molecular motion that cause averaging of the dipolar interactions.

The overall features in the 2D WISE NMR plot for aerogels prepared with different R/C ratios (Figure 3) resemble each other. The methylene 1D ^{1}H spectra for all three aerogels (Figure 3) show a superposition of a narrow (fwhm of 15 kHz) and a broad component (fwhm of 65 kHz), indicating the inhomogeneity in methylene linkages. However, the size of the narrow component relative to that of the broad resonance increases as the R/C ratio increases. Since the narrow component comes from the more mobile parts of the methylene linkages and the broad 1D ^{1}H line width of 65 kHz is from the immobile portion of the linkages, the increased size of these narrow peaks suggests the higher mobility of methylene linkages in aerogels prepared with high R/C ratios. It is understandable that some fraction of the methylene linkages becomes more mobile when the number of linkages per ring or the degree of cross-linkage is reduced. The increase in the mobile component with increased R/C ratio is also in agreement with the observation of a narrow peak at 29 ppm in the ^{13}C NMR spectra (Figure 2) due to the reduced cross-linkage in aerogels prepared with high R/C ratios. Thus, the 2D-WISE NMR combined with solid-state ^{13}C NMR enables us to examine the conformational inhomogeneity in the methylene linkages.

^{129}Xe NMR. 1D ^{129}Xe NMR Spectra of Xenon Adsorbed in RF Aerogels. Representative CF HP ^{129}Xe NMR spectra of xenon adsorbed in RF aerogels with different R/C ratios are shown in Figure 4. At room temperature, the spectra of all samples show two signals of various widths and intensities (the signal at ~0 ppm is from Xe in the gas phase and will not be discussed). The width of the narrower signal for all five materials is close to 1000 Hz. The chemical shift position of the signal depends on the sample and at room temperature is between 85 and 100 ppm. We did not find any apparent correlations between the observed room-temperature shifts and R/C ratio, BET surface area, or the density of the materials. The broader signal is 9.5−11 kHz wide, with its position close to 140 ppm for all samples. The relative intensity of the broader signal at room temperature increases almost linearly with the R/C ratio from about 44 to 57%. The parameters of the room temperature ^{129}Xe NMR spectra are summarized in Table 2. Based on the magnitude of the chemical shifts, one can tentatively assign the narrower signals to xenon residing in the mesoporous spaces and the broader signals to xenon adsorbed in micropores. The observation of the separate signals indicates that the exchange rate between these two regions is slow compared to the chemical shift difference. The width of the observed signals is most likely a reflection of the pore size distributions in different adsorption regions.

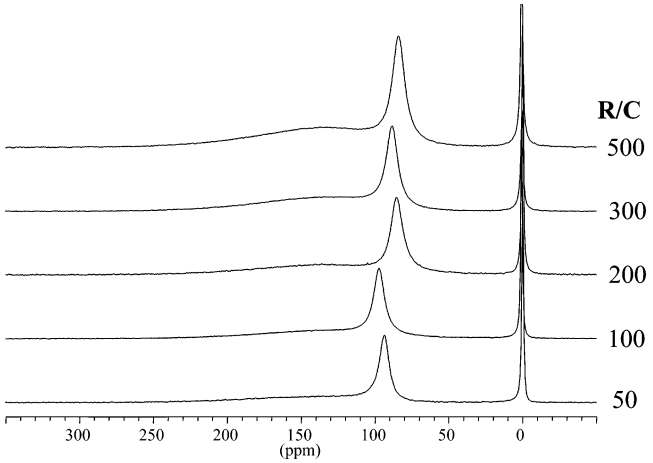

Figure 4. Continuous flow HP ^{129}Xe NMR spectra, at 293 K and a flow rate of 45 sccm, for RF aerogels prepared with different R/C ratios.

TABLE 2: Parameters of ^{129}Xe Spectra in RF Aerogels with Different R/C Ratio

	narrow line			broad line		
R/C	line width,[a] Hz	δ, ppm	integrated intensity,[a] %	line width, Hz	δ, ppm	integrated intensity, %
50	920	93.7	56	9600	144	44
100	977	97.4	52	10200	140	48
200	1070	85.5	50	11000	141	50
300	1020	89.4	44	10200	142	56
500	1080	84.1	43	10400	140	57

[a] The relative intensities of the signals were obtained by deconvoluting the experimental spectra into two Lorentz lines (gas-phase signal excluded) using the WinFit simulation package from Bruker.

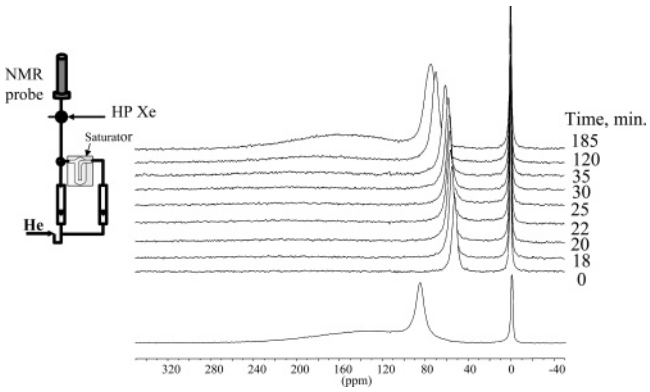

Figure 5. Changes in the ^{129}Xe spectra as a function of time after exposure of the RF aerogel (R/C = 300) to $CHCl_3$ vapor. The bottom spectrum was recorded before the exposure. The spectrum above it was obtained after 5 min of continuous exposure to the stream of helium saturated with the chloroform vapor, and the other spectra were recorded at the times indicated after the delivery of $CHCl_3$ was stopped. The inset shows schematically the apparatus used to deliver the chloroform.

Adsorption of Chloroform in Different Adsorption Regions of RF Aerogels. Adsorption of guest molecules in different adsorption regions of aerogels can be evaluated by mixing molecules of adsorbate (in this case $CHCl_3$) into the carrier gas mixture containing HP xenon. Xe atoms in this case act as a tracer to indicate if some voids become filled with adsorbate. When the voids normally accessible to Xe are occupied by the adsorbed molecules, the signal of Xe can either decrease in intensity, indicating partial occupancy, or completely disappear, if the space is completely blocked. By disconnecting the supply of $CHCl_3$ from the gas stream at a later time, one can also follow the kinetics of desorption of the chloroform.

Figure 5 shows the results of this experiment performed on RF aerogels with R/C = 300. After exposure of RF aerogels to the chloroform the broader signal of adsorbed xenon has completely disappeared. The second ^{129}Xe signal has lost only about one-third of its intensity, become somewhat narrower, and shifted to lower frequencies. The disappearance of the broader signal is due to a complete blocking of some part of the pore space to Xe atoms. This result indirectly confirms our tentative assignment of the broader signal to the micropore space. It is natural to expect that for a material with homogeneous chemical composition of the surface the smaller pores will be filled the first. The shift and contraction of the second ^{129}Xe signal (given the preliminary assignment of xenon residing in the mesopore space) most likely results from a partial or complete blockage of some pore space that contained adsorbed xenon involved in a fast exchange with the gas phase. The experimentally observed direction in the shift would then indicate that now blocked pore space had a smaller size (based on empirical correlations between pore size and ^{129}Xe chemical shifts, see refs 23 and 24 and references therein). Indeed, the observed chemical shift of Xe in fast exchange between pores of different sizes is a weighted sum of the shifts for each type of pore, and exclusion of the smaller pores will reduce the observed value. The reduction in the signal width can be due to either the slowing/eliminating of the exchange or to a narrowing of the distribution of the pore sizes, or perhaps to both. One can also be certain that the observed shift is not caused by the interaction between adsorbed Xe and $CHCl_3$, since such an interaction would cause a shift of opposite sign.[25]

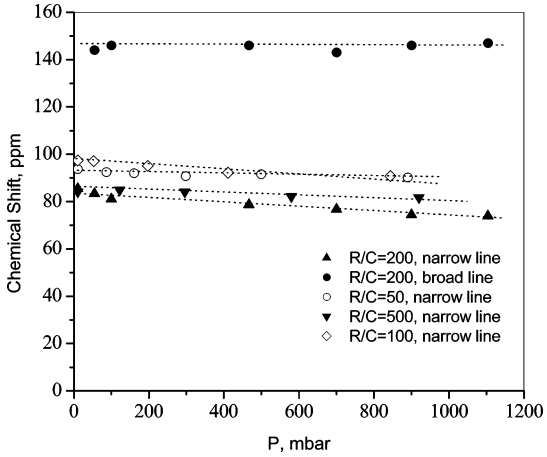

Figure 6. Variation of the ^{129}Xe chemical shifts with pressure, at 293 K, for aerogels with different R/C ratios. The dotted lines are a visual aid only.

Reoccupation of the pore space by Xe as the chloroform desorbs is observed after 20−25 min, and after about 3 h the spectra have returned almost to the original state. The last fact demonstrates that $CHCl_3$ adsorption is completely reversible and that the $CHCl_3$ does not produce permanent modification of the surface.

Variable Pressure ^{129}Xe NMR. The pressure dependence of the chemical shifts for aerogels with different R/C ratios is summarized in Figure 6. The position of the narrow component shifts downfield for the higher loadings for all samples, although the span of the change is slightly different for each material. The largest change in the shift is about 11 ppm, in the pressure range between 10 and 1100 mbar, in the case of R/C = 200. For the other materials, the changes are somewhat smaller. The character of the decrease, however, is similar for all of the samples.

Due to a very low heat of adsorption, the residence time for xenon on the surface is usually very short and, unless the experiment is performed at very low temperature, it is in fast exchange with the gas phase on the scale of the chemical shift differences. The observed ^{129}Xe shift is usually a weighted average between that for xenon adsorbed on the surface and in the gas phase. It has been demonstrated for many materials that when the interaction of xenon with the adsorbent is very weak (i.e., a Henry's law type adsorption isotherm), a pressure dependence of the chemical shift is practically absent.[23−25] When the adsorption isotherm is of the Langmuir type, a small decrease in the chemical shift at higher pressures of xenon[23,26] can be observed. Generally, the variation of the shift in this case does not exceed several ppm.

In situations where stronger adsorption sites, such as dispersed metals[26−28] or charged anionic particles,[29,30] are present on the surface, the variation of the shift with pressure can be quite different. At the lowest xenon pressures, the strongest adsorption

sites are occupied first and cause a higher initial chemical shift. Then, with increasing xenon pressure, only weak sites with lower chemical shifts are occupied. As a result the observed averaged ^{129}Xe shift decreases with increasing equilibrium pressure. For nonmetallic diamagnetic adsorption centers, this can produce a variation of the chemical shift on the order of 10−15 ppm for a range of equilibrium pressures between 0.01 and 1 atm.[30,31]

Interaction between xenon atoms inside the pores can also contribute into the observed ^{129}Xe chemical shift, and depends on xenon concentration, shifting the signals to lower field with higher loading. At very low Xe loading, as in the room-temperature CF experiments, the contribution from the Xe−Xe interactions is insignificant. Only for highly loaded samples, and in CF experiments at very low temperatures, where condensation of xenon is possible, does the effect become appreciable. For xenon pressures of several bars, the δ_{Xe-Xe} contribution can be of the order of a few ppm. Such downfield shifts of the signals due to increased Xe−Xe interaction in the adsorbed layer at low temperature were previously observed on amorphous silica, alumina, and silica−alumina.[31] This effect will depend on the relative diameter of the pores, becoming greater for pores whose size approaches that of the xenon atom.

From the data in Figure 6, it is difficult to conclude whether the observed changes are the result of the presence of a small concentration of strong adsorption centers or whether this is due to Langmuir type adsorption of xenon in all of the materials studied. However, we favor the latter model since we observed a strong deviation of the xenon adsorption isotherms from the Henry's law type toward the Langmuir type at the higher pressures, for all of the materials studied. Note, however, that the range of the chemical shift changes is somewhat greater than expected.

The position of the broader component did not appear to change over the pressure range studied. Note, however, that the accuracy of detection of small changes is rather limited due to the signal width.

Evaluation of Xenon Exchange between Different Porous Regions with 2D EXSY ^{129}Xe NMR. ^{129}Xe 2D EXSY experiments were used to resolve the origin of the signals in the spectra of adsorbed xenon and to evaluate interconnectivity between different adsorption regions in RF aerogels. The 2D EXSY experiments indicate the presence of exchange, the probable exchange pathway, and the time scale of the process. Exchange between regions with different chemical shifts manifests itself in the appearance of cross-peaks between the signals from the sites in exchange. The intensities of the cross-peaks are proportional to the exchange time (τ) set in the experimental pulse sequence. For the sites without exchange, or when the exchange time τ is set to zero, only intensity on the main diagonal will appear in the spectrum. Standard 2D EXSY is a quantitative experiment, allowing estimation of all of the exchange rates. In our case, however, quantification is not feasible because of nonequilibrium polarizations, and the fact that lines are not well resolved. In the past, ^{129}Xe 2D EXSY NMR experiments with thermally polarized xenon were used extensively for evaluation of the exchange between various adsorption sites for Xe in zeolites and other materials.[14−19] The main practical drawback of the technique is that it requires rather long acquisition times. This problem can often be reduced by the use of hyperpolarized xenon. HP Xe is particularly effective in this regard for materials with relatively unrestricted diffusion of xenon and rather long ^{129}Xe relaxation times, which is the case for RF aerogels used in this study.

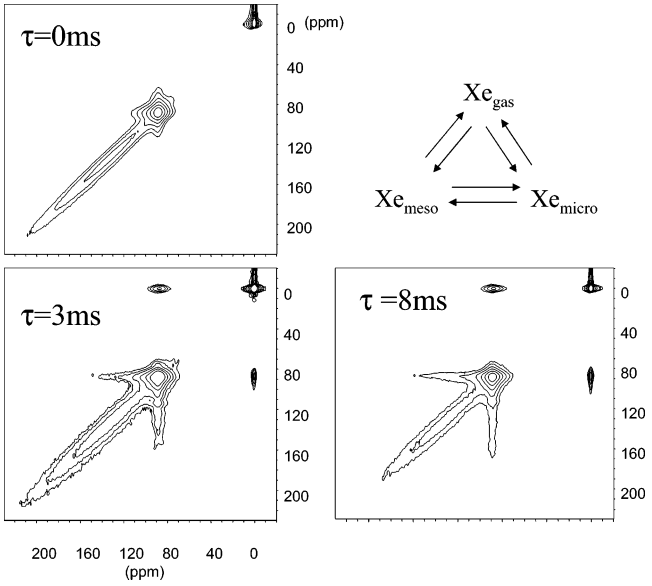

Figure 7. Continuous flow HP 2D EXSY ^{129}Xe NMR spectra, at 293 K, for the RF aerogel (R/C = 300) at different mixing intervals τ. The inset on the right shows the exchange pathways.

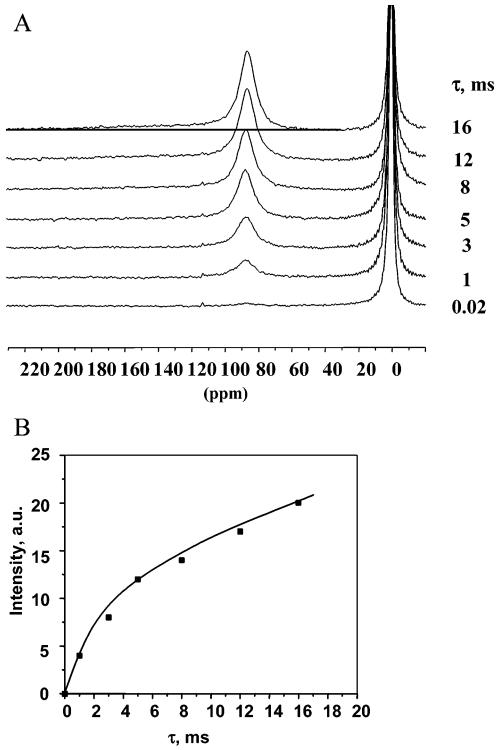

Figure 8. (A) Cross-sections at 0 ppm in the CF 2D EXSY ^{129}Xe spectra, at 293 K, of the RF aerogel (R/C = 300) taken at different mixing intervals τ. (B) Normalized intensity of the cross-peak between gas phase and mesopore signals as a function of τ.

The experimental spectra with different τ for the RF aerogel with R/C = 300 are shown in Figure 7. As expected, with τ = 0 the signals appear only on the main diagonal. Off-diagonal intensities, however, appear even at τ = 0.5ms and become quite pronounced with τ > 1 ms. The 2D EXSY spectra show (and this can be seen even better in the corresponding cross-sections) that on a time scale of a few milliseconds there is exchange between all of the adsorption regions and xenon in the gas phase. Figure 8A shows the cross-sections from the 2D spectra taken in the F2 dimension at 0 ppm, indicating clearly the exchange between all adsorption regions on the millisecond time scale.

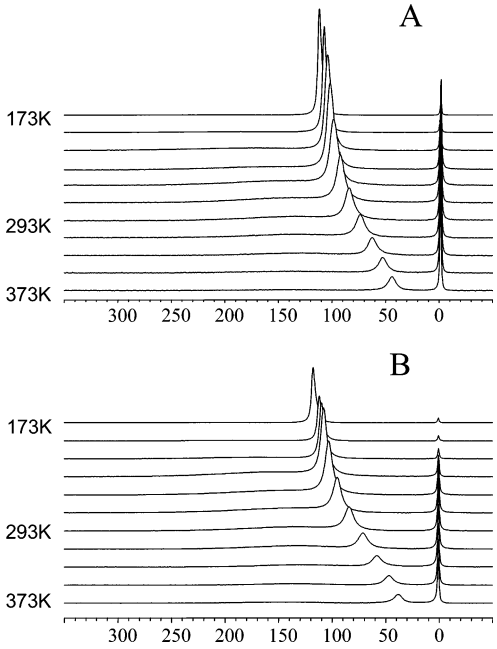

Figure 9. Variable temperature CF HP ^{129}Xe NMR spectra in RF aerogels at 20 K intervals for R/C = 200 (A) and R/C = 500 (B).

The normalized intensity of the cross-signal between the gas-phase signal and the signal assigned to the mesoporous region as a function of τ, Figure 8B, is typical for slow exchange on the chemical shift time scale. Note the striking difference between the shapes of the signals in the 2D spectra. The diagonal signals from the gas phase and from xenon in the mesopores (~90 ppm) each have 2D line shapes with cylindrical symmetry, but the broader component appears as a long and narrow ridge. This feature indicates a broad distribution of adsorption sites with very slow exchange between different parts of this subset.[17,19] Overall, the observed evolution with τ clearly indicates a hierarchical set of exchange processes. The exchange of Xe gas follows the sequence (from fastest to slowest): (i) between mesopores and free gas, (ii) between meso- and micropores, (iii) between micropores and free gas, and (iv) between micropore sites.

2D EXSY data further confirm our original assignment of the narrow and broad signals. The chemical shift value of the narrow signal, its easy exchange with both Xe in the gas phase and xenon producing the broader signal, and the way it is affected by coadsorbed $CHCl_3$ all point to its being due to xenon in the mesopores. The broader signal must then be assigned to Xe adsorbed in micropores formed by agglomerated polymer particles. The large line width is apparently a result of a very broad distribution in the micropore sizes and shapes. The fact that xenon exchange from micropores to the gas phase and to the mesopores is faster than to other micropores suggests that the micropores are distributed homogeneously throughout the material, and that there are no large, separate domains of micropores. In such a situation, the accessible micropores are always open either to mesopores or to free xenon, and it obviously takes longer for a xenon atom to exchange between two different micropores.

Variable Temperature ^{129}Xe NMR. The variable temperature ^{129}Xe NMR spectra, obtained between 173 and 393 K, show similar behavior for all of the materials, with the position and intensity of the narrow component changing the most, Figure 9. Changes in the position of the broad signal become noticeable only below 243 K. The relative intensity of the broad component is at a maximum at around room temperature.

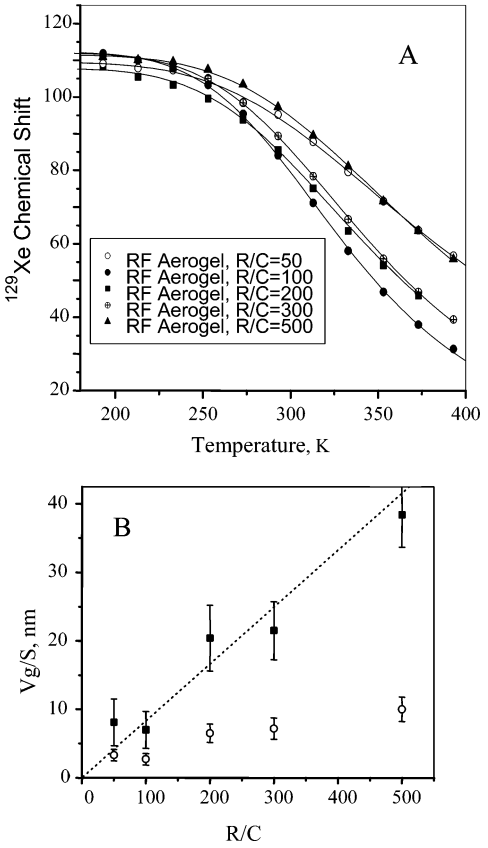

Figure 10. (A) ^{129}Xe chemical shift plotted as a function of temperature for the narrow signal arising from the mesopores in RF aerogels with different R/C ratios. The solid dots are experimental data obtained from CF HP ^{129}Xe NMR spectra recorded at 20 K intervals, and the solid line is the fit using eq 1. (B) The volume to surface-area ratio V_g/S as a function of R/C ratios from Xe NMR (■) and N_2 adsorption data (○).

The temperature dependence of the ^{129}Xe chemical shifts of the narrow component, plotted for all R/C in Figure 10A, is characteristic of the physical adsorption of xenon on solid surfaces, as observed before in numerous micro- and mesoporous materials.[23,24] Using the approach developed previously,[23] one can fit the experimental data to extract the parameters related to the adsorption properties of the materials. In the fast exchange approximation with weak adsorption, the temperature dependence of the observed CS δ for arbitrary pores can be expressed as[23]

$$\delta = \delta_s \left(1 + \frac{V_g}{SK_0RT} e^{\Delta H_{ads}/RT}\right)^{-1} \quad (1)$$

where V_g is the free volume inside the aerogel, S is a specific surface area, K_0 is the pre-exponent of Henry's constant, R is the universal gas constant, ΔH_{ads} is the heat of adsorption, and δ_s is the ^{129}Xe CS characteristic of the surface. K_0 was found from Xe adsorption data (Table 1). δ_s, ΔH_{ads}, and V_g/S were then determined, specifically for the mesopores, from fits of the variable temperature mesopore CS measurements to eq 1, as shown in Figure 10A. All of the ΔH_{ads}'s are close to 20 kJ/mol, consistent with physical adsorption of Xe. The δ_s's are similar for all of the samples and comparable to those normally observed on uncharged surfaces of silica- or silica-organic based materials.[24] A similar analysis for the broad signal from the micropores was not carried out, since this would be somewhat ambiguous due to the fact that the signal represents a distribution of micropores.

The volume-to-surface-area ratios (V_g/S) show a very strong correlation with the R/C ratios (Figure 10B), with an unusually large span in the observed values; an increase in R/C ratio from 50 to 500 inducing a roughly 5-fold rise in the V_g/S's. Since the chemical composition of the surface is practically identical for all of the samples, chemical effects can be ruled out, consistent with the absence of variation in δ_s. It is only the change in the geometry, size, and interconnectivity of the voids that should be responsible for the observed changes in V_g/S. What makes the situation particularly interesting is the magnitude of the V_g/S change. From simple geometrical considerations, one can easily show that the observed changes in V_g/S cannot be reproduced from a single model and will necessarily require some significant rearrangements of the void spaces, whether by some additional connectivity between the pores, changing the shape of the pores or by drastic re-packing of the material framework. As an illustration, in a simple case of cylindrical or slit pores, the interconnection of the pores can increase V_g/S by no more than a factor of 2.[23] Even more advanced models, i.e., a globular model with quite open void space,[31] is unlikely to account for such a large span of V_g/S as observed in the present study. The ratio of total free volume to total surface area obtained from N_2 adsorption data (Figure 10B and Table 1) displays a weaker correlation with the R/C ratio than the V_g/S of the mesoporous space sampled by Xe atoms, indicating that the R/C ratio has a large effect on the mesoporous region.

The increase in V_g/S with R/C in the current system is mainly due to a decrease in the surface of the accessible void space and not due to a decrease in the density of the material. Although the catalyst concentration does have some effect on the density, the latter parameter does not correlate with R/C the same way as V_g/S and, in fact, is practically constant for an R/C ratio above 100.[32] This implies that for materials prepared with smaller R/C ratios the framework will be composed of smaller particles and the accessible voids on the average will be smaller, providing a higher surface area. If the average density remains nearly the same, then an increase in V_g/S with R/C indicates large average particle sizes (and smaller surface area), and on average larger voids as well. These conclusions agree well with TEM data for RF aerogels prepared with different R/C ratios.[32]

Conclusions

Continuous flow hyperpolarized ^{129}Xe NMR in combination with solid-state ^{13}C and two-dimensional wide-line separation (2D-WISE) NMR techniques have been used to study RF aerogels prepared with different [resorcinol]/[catalyst] (R/C) ratios in the starting sol−gel solutions. The degree of polymerization and the mobility of the cross-linking functional groups in RF aerogels were examined and correlated with the R/C ratios. The aerogels with higher R/C ratios have a lower degree of cross-linking and higher mobility in their polymer network. The origin of two different adsorption regions was evaluated using a combination of chloroform coadsorption and 2D EXSY ^{129}Xe NMR. The narrow and broad signals in 1D ^{129}Xe NMR spectra were assigned to meso- and microporosities, respectively. A hierarchy of Xe exchange processes in RF aerogels was demonstrated using 2D EXSY ^{129}Xe NMR. The exchange of Xe gas follows the sequence (from fastest to slowest): mesopores with free gas, gas in meso- and micropores, free gas with micropores, and, finally, among micropore sites. The volume-to-surface-area (V_g/S) ratios for aerogels were estimated for the first time without using any geometric models. The V_g/S parameter, which is related both to the geometry and the interconnectivity of the porous space, has been found to correlate strongly with the R/C ratio and exhibits an unusually large span: an increase in the R/C ratio from 50 to 500 results in a roughly 5-fold rise in V_g/S. Both the V_g/S ratio and the Xe exchange data provide important insights regarding the geometry and the interconnectivity of the nano- and mesoporous spaces in aerogels.

Acknowledgment. This work was partly supported by the Division of Materials Sciences, Office of Basic Energy Sciences, U. S. Department of Energy (USDOE). Partial support for this work also has been provided through the DOE Center for the Synthesis and Processing of Advanced Materials. Pacific Northwest National Laboratory is a multiprogram national laboratory operated for the USDOE by Battelle Memorial Institute under Contract DE-AC06-76RL0 1830.

References and Notes

(1) Pekala, R. W. *J. Mater. Sci.* **1989**, *24*, 3221.
(2) Pekala, R. W.; Alviso, C. T.; Kong, F. M.; Hulsey, S. S. *J. Non-Cryst. Solids* **1992**, *145*, 90.
(3) Pekala, R. W.; Alviso, C. T.; LeMay, J. D. In *Chemical Processing of Advanced Materials*; Hench, L. L., West, J. K., Eds.; J. Wiley & Sons: New York, 1992; p 671.
(4) Kong, F. M.; LeMay, J. D.; Hulsey, S. S.; Alviso, C. T.; Pekala, R. W. *J. Mater. Sci.* **1993**, *8*, 3100.
(5) Lu, X.; Arduini-Schuster, M. C.; Kuhn, J.; Nilsson, O.; Fricke, J.; Pekala, R. W, *Science* **1992**, 225, 971.
(6) Moudrakovski, I. L.; Wang, L.-Q.; Baumann, T.; Satcher, J. H.; Jr.; Exarhos, G. J.; Ratcliffe, C. I.; Ripmeester, J. A. *J. Am. Chem. Soc. Commun.* **2004**, *126*, 5052.
(7) (a)Grover, B. C. *Phys. Rev. Lett*. **1978**, *40*, 391. (b) Happer, W., Miron, E.; Schaefer, S.; Schreiber, D.; van Wingaarden, W. A.; Zeng, X. *Phys. Rev. A* **1984**, *29*, 3092. (c) Driehuys, B.; Cates, G. D.; Miron, E.; K. Sauer; Walter, D. K.; Happer, W. *Appl. Phys. Lett*. **1996**, *69*, 1668.
(8) Werstler, D. D. *Polymer*, **1986**, *27*, 757.
(9) Sebenik, A.; Osredkar, U.; Vizovisek, I. *Polymer* **1981**, *22*, 804.
(10) Clauss, J.; Schmidt-Rohr, K.; Adam, A.; Boeffel, C.; Spiess, H. W.; *Macromolecules* **1992**, *25*, 5208
(11) Schmidt-Rohr, K.; Clauss, J.; Spiess, H. W. *Macromolecules* **1992**, *25*, 3273
(12) Gregg, S. J.; Sing, K. S. W. *Adsorption, Surface Area and Porosity*, 2nd ed.; Academic Press: London, 1982.
(13) W. T. Dixon, *J. Chem. Phys*. **1982**, *77*, 1800.
(14) Larsen, R. G.; Shore, J. S.; Schmidt-Rohr, K.; Emsley, L.; Long, H.; Pines, A.; Janicke, M.; Chmelka, B. F. *Chem. Phys. Lett*. **1993**, *214*, 220.
(15) Kritzenberger, J.; Gaede, H. C.; Shore, J.; Pines, A. *J. Phys. Chem.* **1994**, *98*, 10173.
(16) Moudrakovski, I. L.; Ratcliffe, C. I.; Ripmeester, J. A. *J. Am. Chem. Soc.* **1998**, *120*, 3123.
(17) Moudrakovski, I. L.; Ratcliffe, C. I.; Ripmeester, J. A. *App. Magn. Reson.* **1995**, *8*, 385.
(18) Zhu, X.; Moudrakovski, I. L.; Ripmeester, J. A. *Energy Fuels* **1997**, *11*, 245.
(19) A. Kentgens et al. *Macromolecules* **1991**, *24*, 3712.
(20) A. Bielecki, A.; Burum, D. *J. Magn. Reson*. **1995**, *116*, 215.
(21) Moudrakovski, I.; Lang, S.; Ratcliffe, C. I.; Simard, B.; Santyr, G.; Ripmeester, J. *J. Magn. Reson.* **2000**, *144*, 372.
(22) Moudrakovski, I. L., Sanchez, A. A., Ratcliffe, C. I., Ripmeester J. A. *J. Phys. Chem. B* **2001**, *105*, 12338.
(23) Terskikh, V.; Mudrakovski, I.; Mastikhin, V. *J. Chem. Soc. Faraday Trans.* **1993**, *89*, 4239.
(24) Terskikh, V. V.; Moudrakovski, I. L.; Breeze, S. R.; Lang, S.; Ratcliffe, C. I.; Ripmeester, J. A.; Sayari, A. *Langmuir* **2002**, *18*, 5653.
(25) Conner, W. C.; Weist, E. L.; Ito, T.; Fraissard, J. *J. Phys. Chem*. **1989**, *93*, 4138.
(26) de Menorval, L. C.; Fraissard, J.: Ito, T. *J. Chem. Soc., Faraday Trans*. **1982**, *78*, 403.
(27) Cho, S. J.; Ahn, W. S.; Hong, S. B.; Ryoo, R. *J. Phys. Chem*. **1996**, *100*, 4996
(28) Ryoo, R.; Ko, C. H.; Kim, J. M.; Howe, R. *Catal. Lett.* **1996**, *37*, 29.
(29) Terskikh, V. V.; Mastikhin, V. M.; Timofeeva, M. N.; Okkel, L. G.; Fenelonov, V. B. *Catal. Lett*. **1996**, *42*, 99.
(30) Cheung, T. T. P. *J. Phys.Chem.***1989**, *93*, 7549.
(31) Karnaukhov, A. P. *Kinet. Katal*. **1971**, 12, 1025.
(32) LeMay, J. D.; Hopper, R. W.; Hrubesh, L. W.; Pekela, R. W. *MRS Bulletin*, **1990**, *15*, 30.